THE SIGNIFICANCE OF NEAR-FAULT EFFECTS ON LIQUEFACTION

R.A. Green[1], J. Lee[2], T.M. White[3], and J.W. Baker[4]

[1] *Associate Professor, Dept. of Civil and Environmental Engineering, Virginia Tech, Blacksburg, VA, USA*
Email: rugreen@vt.edu
[2] *Doctoral Candidate, Dept. of Civil and Environmental Engineering, University of Michigan, Ann Arbor, MI, USA*
[3] *Instructor, Dept. of Civil and Environmental Engineering, US Air Force Academy, USAF Academy, CO, USA*
[4] *Assistant Professor, Dept. of Civil and Environmental Engineering, Stanford University, Stanford, CA, USA*

ABSTRACT :

The objective of the study presented herein is to access the influence of rupture directivity on the inducement of liquefaction in loose, saturated sand. Rupture directivity is a near fault phenomenon that results in a pronounced double-sided velocity pulse in the strike normal component(s) of motion. Using the Palmgren-Miner fatigue theory, implemented for low cycle fatigue conditions, the number of equivalent cycles were computed for twenty seven sets of strike normal and strike parallel components of motions, where the former components had the pronounced velocity pulses and the latter did not. Using these results and other results from site response analyses, the cyclic stress ratios adjusted to M7.5 were computed for both components of motions in a soil profile at a depth corresponding to ~1 atm of effective vertical stress. Two clear trends where identified. First, the strike normal components tended to induce larger cyclic stresses in the soil than the strike parallel components. However, the strike normal components of motions had fewer numbers of equivalent cycles as compared to the strike parallel components. Although these trends are somewhat compensating in their influence on the inducement of liquefaction, the net result was that the motions containing the rupture directivity pulses had a slightly larger potential to induce liquefaction than motions without the pulses.

KEYWORDS: liquefaction, near-fault effects, rupture directivity, directivity, number of equivalent cycles

1. INTRODUCTION

The objective of the study presented herein is to access the influence of "rupture directivity" on the inducement of liquefaction in loose, saturated sand. Rupture directivity (or "directivity") is one of two phenomena that can result in a pronounced velocity pulse in near-fault motions; the other phenomenon is referred to as "fling step" or "fling" and is not considered in this paper. Directivity is a Doppler-type phenomenon resulting from the approximate equality of the fault rupture and shear wave velocities and can result in a double-sided velocity pulse in the strike normal component(s) of motion. Several studies have examined the detrimental effects of near fault motions on building structures (e.g., Hall et al., 1995; Sasani and Bertero, 2000; Alavi and Krawinkler, 2001; Makris and Black, 2003; and Luco and Cornell, 2007), but relatively little attention has been given to near fault effects on liquefaction.

To assess the influence of rupture directivity on the inducement of liquefaction, a series of site response analyses were performed to determine the cyclic stress ratios (CSR) at depth in a soil profile. The input motions used in the analyses consisted of twenty seven sets of strike normal and strike parallel components of motions, for a total of 54 motions and site response analyses. The strike normal component of each set of motions was identified as having velocity pulses that are likely due to rupture directivity, while the strike parallel component

had no identifiable velocity pulse. To account for the influence of ground motion duration on the inducement of liquefaction, the number of equivalent cycles were computed for all the motions using the Palmgren-Miner fatigue theory, implemented for low cycle fatigue conditions (Green and Terri, 2005), and motion specific magnitude scaling factors (MSFs) determined. This allowed the cyclic stress ratios adjusted to M7.5 (i.e., $CSR_{M7.5}$) for the strike normal and strike parallel components for each set of motions to be computed and compared and the influence of near fault directivity effects to be discerned.

In the subsequent sections of the paper, first the criteria used to select the ground motions included in this study are discussed. Next, an overview of the site response analyses is presented and trends in the resulting CSRs are discussed. This is followed by a presentation and discussion of the number of equivalent cycles for the motions and the corresponding motion specific MSFs. Finally, the $CSR_{M7.5}$ for the strike normal and strike parallel motions are compared and the influence of near-fault directivity on the inducement of liquefaction is discussed.

2. SELECTION OF GROUND MOTIONS

As stated above, twenty seven sets of strike normal and strike parallel motions were used in this study. These motions were selected from a database of ninety one sets of strike normal and strike parallel motions, where all the strike normal components in the database were previously identified as being "pulse-like" by Baker (2007); a "pulse-like" motion is one that has pronounced velocity pulse, which may or may not be due to near fault effects. To select the sets of motions believed to contain rupture directivity effects, first a visual comparison of the strike normal and strike parallel velocity time histories was made. Although somewhat subjective, in general, a set of motions was considered to contain directivity effects if the strike normal component was pulse-like, but the strike parallel component was not. The basis for this selection criterion is that rupture directivity will only result in a pronounced velocity pulse in the strike normal component(s), not in the strike parallel component. Next, all ninety one set of motions were evaluated using the following predictive equation (Baker, 2007):

$$PI = \frac{1}{1+e^{-23.3+14.6\cdot pgv_{ratio}+20.5\cdot energy_{ratio}}} \qquad (2.1)$$

where, in this study: PI = pulse indicator ($0<PI<1$); pgv_{ratio} = the ratios of the peak ground velocities of the strike parallel and strike normal components of motion; and $energy_{ratio}$ = the ratio of the cumulative squared velocities of the strike parallel and the strike normal components of motion. For a set of motions, the closer PI is to unity, the more likely the motions contain directivity effects; sets of motions having $PI \geq 0.85$ were classified as having rupture directivity effects.

Baker (2007) originally developed Eqn. 2.1 and the $PI \geq 0.85$ criterion for identifying pulse-like motions, where he computed pgv_{ratio} and $energy_{ratio}$ using the "residual" motion in lieu of the strike parallel motion (the residual motion is the strike normal component of motion with the velocity pulse removed). However, with the exception of one set of motions, the initial visual classification and Eqn. 2.1, as implemented in this study, yielded the same results. And, upon a second visual inspection, the one set of motions in contention was reclassified as containing directivity effects. In total, forty two sets of motions were classified as having directivity effects.

The final criterion used to select sets of motions for this study had nothing to do with the rupture directivity phenomenon, but rather, relates to the limitations of the constitutive model used in the site response analyses. Of the forty two sets of motions classified as having directivity effects, only those sets where both components had peak ground accelerations less than 0.5g (i.e., pga < 0.5g) were used. In total, twenty seven of the original ninety one sets of motions met all the selection criteria and were used as input motions in site response analyses to compute the cyclic stress ratios (CSR) at depth in a soil profile. Table 1 lists the selected motions.

Table 1. Sets of motions selected for use in this study.

No.	Event	Year	Station	M_w	Distance* (km)
1	Coyote Lake	1979	Gilroy Array #6	5.7	3.1
2	Imperial Valley-06	1979	Aeropuerto Mexicali	6.5	0.3
3	Imperial Valley-06	1979	Agrarias	6.5	0.7
4	Imperial Valley-06	1979	EC Meloland Overpass FF	6.5	0.1
5	Imperial Valley-06	1979	El Centro Array #4	6.5	7.1
6	Imperial Valley-06	1979	El Centro Array #6	6.5	1.4
7	Imperial Valley-06	1979	El Centro Array #7	6.5	0.6
8	Morgan Hill	1984	Gilroy Array #6	6.2	9.9
9	Taiwan SMART1 (40)	1986	SMART1 C00	6.3	-
10	Taiwan SMART1 (40)	1986	SMART1 M07	6.3	-
11	Whittier Narrows-01	1987	Downey-company maintenance bldg	6.0	20.8
12	Whittier Narrows-01	1987	LB-Orange Ave.	6.0	24.5
13	Superstition Hills-02	1987	Parachute Test Site	6.5	1.0
14	Loma Prieta	1989	Gilroy Array #2	6.9	11.1
15	Loma Prieta	1989	Oakland – Outer Harbor Wharf	6.9	74.3
16	Loma Prieta	1989	Saratoga – Aloha Ave.	6.9	8.5
17	Erzican, Turkey	1992	Erzincan	6.7	4.4
18	Landers	1992	Barstow	7.3	34.9
19	Landers	1992	Yermo Fire Station	7.3	23.6
20	Kocaeli, Turkey	1999	Gebze	7.5	10.9
21	Chi-Chi, Taiwan	1999	TCU075	7.6	0.9
22	Chi-Chi, Taiwan	1999	TCU103	7.6	6.1
23	Chi-Chi, Taiwan	1999	TCU128	7.6	13.2
24	Northwest China-03	1997	Jiashi	6.1	-
25	Chi-Chi, Taiwan-03	1999	CHY080	6.2	22.4
26	Chi-Chi, Taiwan-03	1999	TCU076	6.2	14.7
27	Yountville	2000	Napa Fire Station #3	5.0	-

*Closest distance to the ruptured area on the fault

3. SITE RESPONSE ANALYSES AND CSR

A series of site response analyses were performed using the motions discussed above and CSRs were computed at a depth corresponding to ~1atm vertical effective stress. The shear wave velocity profile for the soil profile used in the site response analyses is shown in Figure 1. The site response analyses were performed using a modified version of SHAKE91 (Idriss and Sun, 1992), with the nonlinear soil characteristics modeled using effective-stress-dependent shear modulus and damping degradation curves proposed by Ishibashi and Zhang (1993). All the motions were treated as rock outcrop motions at bedrock, irrespective of the actual site conditions at the recording seismograph stations.

For each of the analyses, the maximum shear stress (τ_{max}) induced in the soil at a depth of ~7.3m (i.e., the depth corresponding to ~1atm vertical effective stress (σ'_{vo})) was obtained and used to compute the CSR (e.g., Youd et al., 2001):

$$CSR = 0.65 \cdot \frac{\tau_{\max}}{\sigma'_{vo}} \tag{3.1}$$

A plot of the CSRs induced by the strike normal motions versus those for the corresponding strike parallel motions is shown in Figure 2a. As may be observed from this figure, the strike normal CSRs are generally larger than those for the strike parallel motions, and in some cases significantly so. Furthermore, as may be

inferred from Figure 2b, this trend is not simply due to the strike normal input motions having higher pga's than those for the corresponding strike parallel input motions, as the disparity CSRs is more significant than the disparity in the pga's. Rather, the disparity in the CSRs is likely attributed to the rupture directivity velocity pulse in the strike normal motions. Finally, although Figure 2a shows that the strike normal motions tend to induce larger CSRs than the corresponding strike parallel motions, this does not necessarily imply that the former have greater potential to induce liquefaction than the latter, because no consideration has been given to the duration of the respective motions. Duration effects are addressed in the next section.

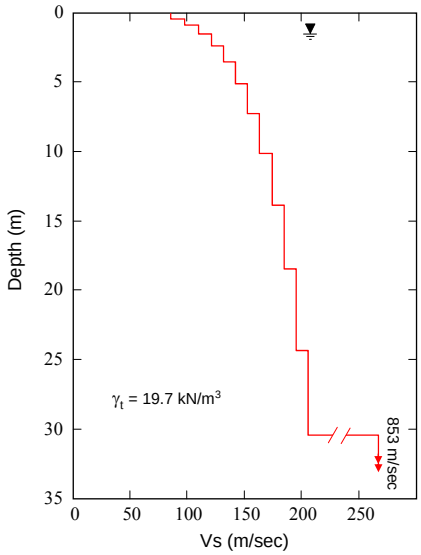

Figure 1. Shear wave velocity profile for the soil profile used in the site response analyses

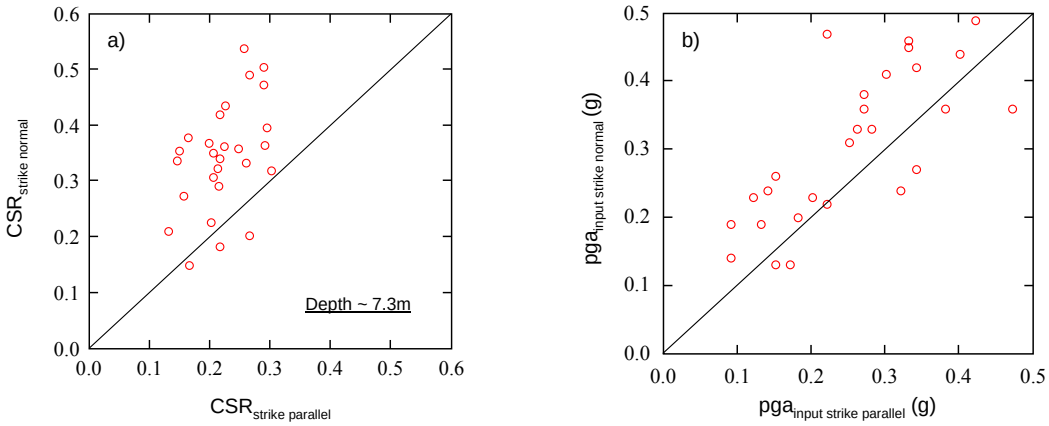

Figure 2. a) Strike normal CSRs vs. strike parallel CSRs for ~7.3m depth; and b) strike normal pga's of input motions vs. strike parallel pga's.

4. DURATION EFFECTS

Per the simplified liquefaction evaluation procedure (e.g., Youd et al., 2001), the influence of ground motion duration on the inducement of liquefaction is accounted for via magnitude scaling factors (MSFs), which can be computed using the equivalent-number-of-cycles concept (e.g., Green, 2001). In this vein, the number of equivalent cycles (n_{eqv}) were computed for all the motions using the Palmgren-Miner fatigue theory, implemented for low cycle fatigue conditions (Green and Terri, 2005). In this approach, n_{eqv} is computed using the following relation:

$$n_{eqv} = \frac{\sum_i \omega_i}{\omega_{ref\,(1cycle)}} \tag{4.1}$$

where, the numerator in this expression is the energy dissipated in a unit volume of soil at a specified depth due to the passage of the ground motions, which is equal to the cumulative area bound by the shear stress – shear strain hysteretic loops obtained from the site response analyses. And, the denominator of this expression (i.e., $\omega_{ref\,(1\ cycle)}$) is the energy that would be dissipated in the same unit volume of soil if it were subjected to one cycle of sinusoidal loading having an amplitude equal to $0.65\times\tau_{max}$. These two quantities are illustrated in Figure 3.

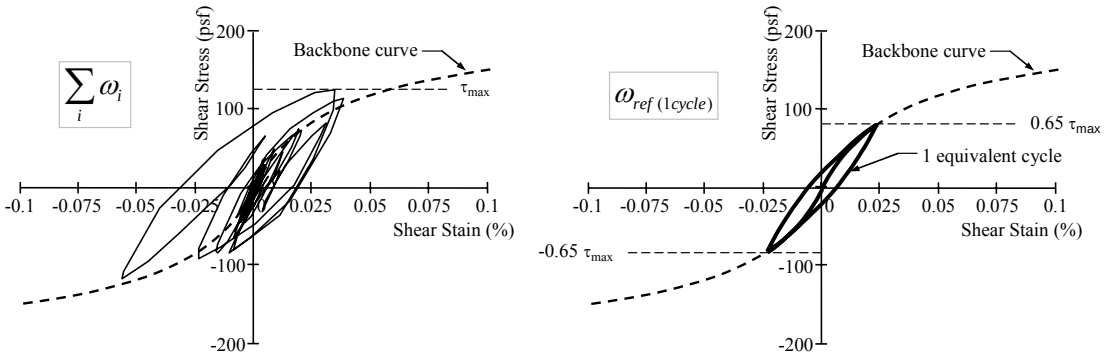

Figure 3. Graphical illustration of the numerator and denominator of Eqn. 4.1.

Figure 4 is a plot of the computed n_{eqv} values for a depth of ~7.3m. As may be observed from this figure, the strike normal motions tend to have fewer cycles than the corresponding strike parallel motions. This trend is somewhat surprising but is consistent with the findings of Somerville et al. (1997) who found that the duration of motions having rupture directivity effects tend to have shorter durations than motions without these effects.

Also shown in Figure 4 are contours of number of equivalent cycles for various site-to-source distances ®, defined as the closest distance to the fault, computed using a predictive relation developed by Lee and Green (2008), which does not account for near fault effects. Although the site-to-source distances for the motions used in this study vary (Table 1), the contours are reasonably representative of the n_{eqv} for the strike parallel motions, but over predict n_{eqv} for the strike normal motions.

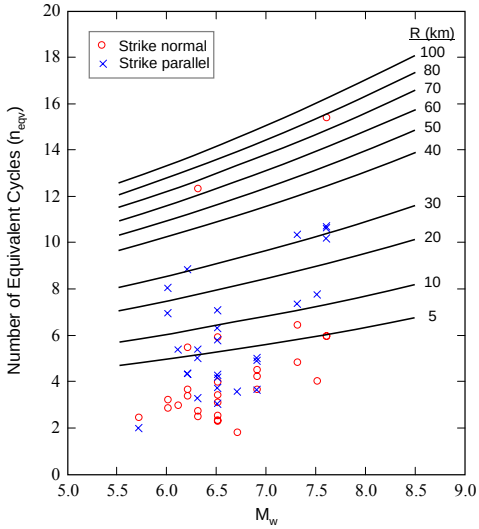

Figure 4. n_{eqv} for the strike normal and strike parallel motions vs. magnitude, and n_{eqv} contours for various site-to-source distances computed using a predictive relation by Lee and Green (2008).

Having the n_{eqv} values, motion specific magnitude scaling factors (MSFs) can be computed using the following relation (e.g., Green, 2001):

$$MSF = \left(\frac{n_{eqv\,M=7.5,R=80km}}{n_{eqv}} \right)^{m} \tag{4.2}$$

where, $n_{eqv\ M=7.5,\ R=80km} = n_{eqv}$ for a "far field" motion from a M7.5 earthquake ("far field" is assumed in this study to be ~80 km); and m is an empirical constant determined from various laboratory studies to range from ~0.2 to ~0.34. For this study, $n_{eqv\ M=7.5,\ R=80km}$ = 14.7 cycles and m = 0.22 where used to compute the motion specific MSFs. The former parameter value was determined using the predictive relation developed by Lee and Green (2008) and is consistent with n_{eqv} = 15 cycles for a M7.5 proposed by Seed and Idriss (1982). The latter parameter value was determined by an iterative approach where the largest value of m was selected that resulted in matching trends in $\sum\omega_i$ and CSRs adjusted to a M7.5 (i.e., $CSR_{M7.5}$) with depth in the soil profile. The resulting value of m = 0.22 falls within the experimentally determined range noted above. The motion specific MSFs are plotted in Figure 5. Also plotted in this figure, is the range of MSFs recommended by Youd et al. (2001)

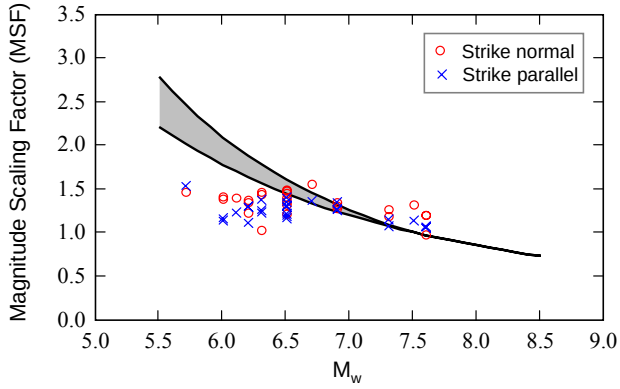

Figure 5. Motion specific MSFs and the range of MSFs recommended by Youd et al. (2001).

As may be observed from Figure 5, the MSFs for the strike normal motions are generally less than those for the strike parallel motions. Also, as may be observed from this figure, the motion specific MSFs for both the strike normal and strike parallel motions fall below the range recommended by Youd et al. (2001) at lower magnitudes. This results from several factors, but is primarily due to the MSFs recommended by Youd et al. being site-to-source independent.

5. NEAR FAULT DIRECTIVITY EFFECTS ON LIQUEFACTION

Up to this point, two opposing trends have been identified regarding the influence of rupture directivity on liquefaction. First, it was shown that directivity tends to result in an increase in the CSR induced in the soil (i.e., increasing the potential to induce liquefaction). Second, it was shown that directivity tends to result in motions having few number of cycles, or correspondingly, higher MSFs (i.e., decreasing the potential to induce liquefaction). The net effect of these two opposing trends can be examine by comparing the CSRs adjusted to M7.5 (i.e., $CSR_{M7.5}$) for the strike normal and strike parallel motions. CSR, MSF, and $CSR_{M7.5}$ are related by the following expression (e.g., Youd et al., 2001):

$$CSR_{M\,7.5} = CSR \cdot \frac{1}{MSF} \tag{5.1}$$

The resulting $CSR_{M7.5}$ induced in the soil profile at a depth of ~7.3m for the strike normal and stike parallel motions are plotted in Figure 6. As may be observed from this figure, the strike normal $CSR_{M7.5}$ tend to be larger than the corresponding strike parallel values, implying that near fault directivity does increase the potential to induce liquefaction. However, the trend is not nearly as pronounced as that for CSR (Figure 2a).

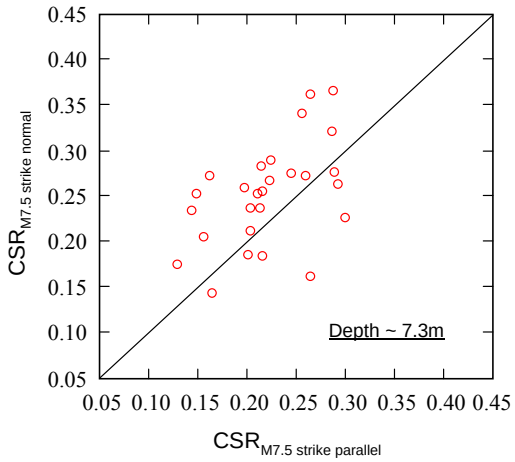

Figure 6. $CSR_{M7.5}$ for strike normal motions vs. $CSR_{M7.5}$ for strike parallel motions

6. CONCLUSIONS

From the analysis of twenty seven sets of strike normal and strike parallel ground motions, where the former component had a pronounced velocity pulse due to rupture directivity and the latter did not, two opposing trends were identified relating to the potential of these motions to induce liquefaction. First, the strike normal components tended to induce larger cyclic stresses in the soil than the strike parallel components. However, the strike normal components of motions had fewer numbers of equivalent cycles, or correspondingly, higher MSFs, as compared to the strike parallel components. These trends are somewhat self compensating in their influence on the inducement of liquefaction, and the net result was that the motions containing the rupture directivity pulses had a slightly larger potential to induce liquefaction than motions without the pulses, as determined by comparing the $CSR_{M7.5}$ for the respective motions. Finally, the authors caution that these findings, while arrived at via a logical process, should be viewed as preliminary until they are rigorously tested by a detailed laboratory study and/or field observations.

ACKNOWLEDGEMENTS

The authors gratefully acknowledge the efforts of Ms. Kate Gunberg and Ms. Stephanie Makowski in down loading the ground motions used in this study and in helping to prepare the input files for the site response analyses. This material is based upon work supported, in part, by the National Science Foundation under Grant No. CMMI 0644580. Any opinions, findings, and conclusions or recommendations expressed in this material are those of the authors and do not necessarily reflect the views of the National Science Foundation.

REFERENCES

Alavi, B. and Krawinkler, H. (2001). Effects of Near-Fault Ground Motions on Framed Structures, Blume Center Report 138, Stanford, CA, USA.

Baker, J.W. (2007). Quantitative Classification of Near-Fault Ground Motions. *Bulletin of the Seismological*

Society of America **97:5**, 1486-1501.

Green, R.A. (2001). Energy-Based Evaluation and Remediation of Liquefiable Soils. Ph.D. Dissertation, Department of Civil and Environmental Engineering, Virginia Tech, Blacksburg, VA, USA.

Green, R.A. and Terri, G.A. (2005). Number of Equivalent Cycles Concept for Liquefaction Evaluations – Revisited. *ASCE Journal of Geotechnical and Geoenvironmental Engineering* **131:4**, 477-488.

Hall, J.F., Heaton, T.H., Halling, M.W., and Wald, D.J. (1995). Near-Source Ground Motions and Its Effects on Flexible Buildings. *Earthquake Spectra* **11:4**, 569-605.

Idriss, I.M. and J.I. Sun (1992). SHAKE91: A Computer Program for Conducting Equivalent Linear Seismic Response Analyses of Horizontally Layered Soil Deposits. University of California at Davis, Davis, CA, USA.

Ishibashi, I. and X. Zhang (1993). Unified Dynamic Shear Moduli and Damping Ratios of Sand and Clay. *Soils and Foundations* **33:1**, 182-191.

Lee, J. and Green, R.A. (2008). Predictive Relations for Number of Equivalent Stress Cycles, *in preparation*.

Luco, N. and Cornell, C.A. (2007). Structure-Specific Scalar Intensity Measures for Near-Source and Ordinary Earthquake Ground Motions. *Earthquake Spectra* **23:2**, 357-392.

Makris, N. and Black, C. (2003). Dimensional Analysis of Inelastic Structures Subjected to Near Fault Ground Motions, Earthquake Engineering Research Center, EERC 2003-05, Berkeley, CA, USA.

Sasani, M. and Bertero, V.V. (2000). Importance of Severe Pulse-Type Ground Motions in Performance-Based Engineering: Historical and Critical Review. *Proc. 12th World Conf. on Earthquake Engineering*, Auckland, New Zealand.

Seed, H.B. and Idriss, I.M. (1982). Ground Motions and Soil Liquefaction During Earthquakes, Earthquake Engineering Research Institute, Oakland, CA, USA.

Somerville, P.G., Smith, N.F., Graves, R.W., and Abrahamson, N.A. (1997). Modification of Empirical Strong Ground Motion Attenuation Relations to Include the Amplitude and Duration Effects of Rupture Directivity. *Seismological Research Letters* **68:1**, 199-222.

Youd, T.L., Idriss, I.M., Andrus, R.D., Arango, I., Castro, G., Christian, J.T., Dobry, R. Finn, W.D.L., Harder, L.F., Hynes, M.E., Ishihara, K., Koester, J.P., Liao, S.S.C., Marcuson, W.F., Martin, G.R., Mitchell, J.K., Moriwaki, Y., Power, M.S., Robertson, P.K., Seed, R.B., and Stokoe, K.H. (2001). Liquefaction Resistance of Soils: Summary Report from the 1996 NCEER and 1998 NCEER/NSF Workshops on Evaluation of Liquefaction Resistance of Soils. *Journal of Geotechnical and Geoenvironmental Engineering* **127:4**, 297-313